Effects of magnons on spin transport in ferromagnetic metals

Bachelor Thesis by:
Alex Cleton, 3869911

University of Utrecht, Netherlands
Faculteit Bètawetenschappen
Natuur- Sterrenkunde

Supervisor:
Dr. R.A. Duine
ITF Utrecht

June 16, 2015

In this Thesis, spin-injection from a ferromagnetic to a non-ferromagnetic region is discussed using drift-diffusion theory. This is an important subject in spintronics nowadays where the spin of the electron is used instead of its charge. First, a simple system with a charge current density is presented. Then, spin-injection due to a constant temperature gradient is studied. Magnons are then brought into this system to see what effect they have. The contribution of the magnons is found to be substantial and results in injected spin accumulations that are $\sim 10^2$ higher than without magnons. We also study the temperature dependence to see in what temperature regimes magnons and electrons are important. At low temperatures, magnons seems to have the biggest contribution.

Contents

1 Introduction

Spintronics became popular in the late 1970s when scientists experimented with transport in various ferromagnetic and non-ferromagnetic materials. The word spintronics is short for spin electronics. Electronics nowadays uses the charge of the electron to power computers etcetera, where in spintronics, the focus is on the spin of an electron and what you can do with it.[1]

In quantum mechanics, a particle has two kinds of angular momenta, the orbital angular momentum (L) and the spin angular momentum (S). To visualize this, consider the Earth's motion around the Sun, where the Earth is the electron and the Sun the nucleus of an atom. The Earth's orbit around the Sun is the orbital angular momentum. The Earth also spins around its own axis, which can be seen as the spin angular momentum. In quantum mechanics, these angular momenta are described by so-called quantum numbers and they can take several different values depending on which kind of particle is described.

Any particle can be in different states and so does the electron. These states can be split into an orbital part and a spin part. The spin part is described by the spin quantum number (s) and the spin projection quantum number (m_s). Because the electron has a spin quantum number of $1/2$ and m_s can take values from $-s$ to s with steps of one, we see that there are 2 possible values for m_s. These states for the electron are called spin up ($\uparrow$) and spin down ($\downarrow$). Now that we know these two states of the electron, we need to use this if we want to describe systems that contain electrons.

In this Thesis, I am going to look at very simple bilayer systems, one side being ferromagnetic (F-side) and the other non-ferromagnetic (N-side). Due to different current polarizations between the ferromagnetic and the non-ferromagnetic side, a spin accumulation builds up at the interface between the two metals. The chemical potential profiles of the spin up and down electrons describe this spin accumulation and are found, together with the spin current density. Different situations are modelled to see what the similarities and differences are. The main aim of this Thesis is to see what happens if magnons are thrown into the equation.

Magnons are so-called quasiparticles. This concept was introduced in 1930 by F. Bloch. When temperature increases, the magnetization decreases because the spin particles deviate from perfect alignment which is the case at zero kelvin. In ferromagnetic materials, the magnetism originates mainly from the magnetic dipole moments of the electrons. Because most of the electrons are aligned (most of them are spin up or spin down), every individual little

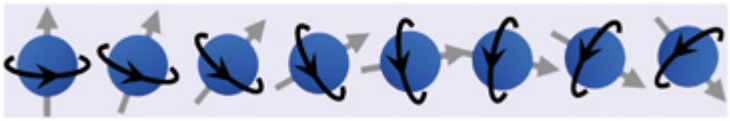

Figure 1: Different spin orientations. Source[2]

magnetic dipole adds up to a macroscopic magnetic field. So the material's magnetic field depends on the alignment of the electrons. If the temperature rises, all these electrons get a certain orientation, a fluctuation from their equilibrium point. In other words, they are not perfectly aligned anymore. These orientations can influence the other spin particles around them and therefor, a certain orientation can propagate through the material like a wave. This is called a magnon. This is comparable with phonons. Particles in a lattice can vibrate a bit and when they do, it also influences the other particles around it. These vibrations propagate through materials like a wave, thus very similar to magnons.

The spin transport drift-diffusion equations are numerically solved to model the different cases. After recalling some basics, the following cases will be discussed:

- Spin-injection due to a charge current density
- Spin-injection due to a temperature gradient
- Only magnons at F-side, electrons at N-side
- Magnons and electrons at F-side, electrons at N-side

Finally the Seebeck coefficient is taken temperature dependent to see at what temperature range electrons and magnons are important, albeit that many assumptions have to be made in this Thesis due to the complexity of real systems. An Appendix is presented at the end of the Thesis containing all the constants used and figures made for the different cases.

2 Theory

2.1 System setup

In this Thesis, only systems with two sides are looked into, a ferromagnetic (F) and a non-ferromagnetic (N) side. For simplicity, we assume the metals are infinitely large, so that we only have to look at one dimension due to translational symmetries in the other directions. The F-side ($x \in [-\infty, 0]$) consists of $Ni_{80}Fe_{20}$, or for short it is called permalloy Py. The N-side ($x \in [0, \infty]$) is made of copper Cu. The interface between these two metals is at $x = 0$.

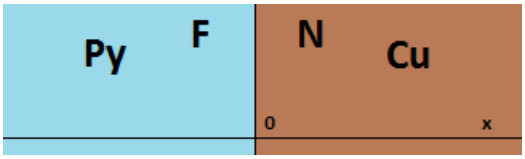

Figure 2: System setup

In all the different scenarios, we will look at how the chemical potentials will look like. These chemical potentials tells us much about the transport of magnetic moments in the non-ferromagnetic region. Due to a charge current or a temperature gradient, these magnetic moments can be transported from the ferromagnet to the N-side of the system. This process is called spin-injection[3]. With the addition of magnons later on, it is interesting to see what happens to this spin-injection that is quantified by the spin accumulation μ_s. This accumulation is just the difference between the chemical potentials of the spin up and down electrons $\mu_\uparrow - \mu_\downarrow$ and comes from the different spin up and down current densities. In the next section, these current densities are explained.

2.2 Current densities

To describe systems with ferromagnetic materials, the drift-diffusion theory is used. There are three kinds of current densities (current divided by area) that are described within this theory. One of them, the heat current density Q, will be ignored entirely in this Thesis. This heat current depends on the heat conductivity and on so-called Peltier coefficients that describe the transport of heat through two different materials when electrical current is

sent through. I will only model scenarios when there is no electrical current at all (except the first most simplest case), so it can be ignored.

The two other current densities are the charge current density j_e and the spin current density j_s which consists of currents being carried by the spin up and spin down electrons, $j_\uparrow$ and $j_\downarrow$. Hence, we have that

$$j_e = j_\uparrow + j_\downarrow, \tag{1}$$

$$j_s = j_\uparrow - j_\downarrow, \tag{2}$$

$$j_\uparrow = \sigma_\uparrow(E - \frac{\nabla\mu_\uparrow}{e}) - \sigma_\uparrow S_\uparrow \nabla T_\uparrow, \tag{3}$$

$$j_\downarrow = \sigma_\downarrow(E - \frac{\nabla\mu_\downarrow}{e}) - \sigma_\downarrow S_\downarrow \nabla T_\downarrow. \tag{4}$$

In the formulas above, $\sigma_\uparrow$ and $\sigma_\downarrow$ are the spin-dependent electrical conductivities of a certain material measured in siemens per meter. Siemens is the inverse of ohm and in SI-units one siemens is equal to $kg^{-1}\ m^{-2}\ s^3\ A^2$, which respectively reads kilogram, meter, second and ampere. Furthermore, E is the external electric field in volt per meter where volt is $kg\ m^2\ A^{-1}\ s^{-3}$. The elementary charge e is measured in coulomb. We also have $S_\uparrow$ and $S_\downarrow$ which are the spin-dependent Seebeck coefficients in volt per kelvin. The temperatures of the spin up and spin down electrons, $T_\uparrow$ and $T_\uparrow$, are in kelvin and $\mu_\uparrow$ and $\mu_\downarrow$ are the spin-dependent electrochemical potentials in joule. The gradients can be seen as m^{-1}. Once these units are plugged into the formulas, one can see the charge and spin current densities, j_e and j_s, are in ampere per square meter, which is exactly what you would expect. If desired, $\nabla\mu_\uparrow/e$ and $\nabla\mu_\downarrow/e$ can also be written as a voltage gradient $\nabla V_\uparrow$ and $\nabla V_\downarrow$ because joule/coulomb is equal to volt.

Now the current density formulas are known, the charge conservation law,

$$\frac{\partial\rho}{\partial t} + \nabla j_e = 0, \tag{5}$$

can help to solve these equations. The first term is the change of the free electric charge densities ρ over time. We assume to be in a steady state so that the first term can be taken zero for our system. One finds that it is best to write the chemical potentials the same way as the current densities,

$$\mu_e = \mu_\uparrow + \mu_\downarrow, \tag{6}$$

$$\mu_s = \mu_\uparrow - \mu_\downarrow, \tag{7}$$

where μ_s is again the spin accumulation. With use of the Valet-Fert equation which describes spin diffusion,[4]

$$\nabla^2 \mu_s = \frac{\mu_s}{\lambda_{sr}^2}, \tag{8}$$

where λ_{sr} is the spin relaxation length of the material, these problems can be solved. The relaxation length tells us to what lengthscale the system goes to equilibrium. With these two differential equations, basic formulas for $\mu_\uparrow$ and $\mu_\downarrow$ can be formed. This leads to many constants that have to be solved with some boundary conditions that can differ a bit for each new case.

2.3 Solving and boundary conditions

With the help of our two differential equations from the previous section we can construct solutions for $\mu_{\uparrow,\downarrow}$. The charge conservation law leads to,

$$\nabla^2(\sigma_\uparrow \mu_\uparrow + \sigma_\downarrow \mu_\downarrow) = 0, \tag{9}$$

and the Valet-Fert equation to,

$$\nabla^2(\mu_\uparrow - \mu_\downarrow) = \frac{(\mu_\uparrow - \mu_\downarrow)}{\lambda_{sr}^2}, \tag{10}$$

where the gradients are just $\frac{d^2}{dx^2}$ and $\mu_{\uparrow,\downarrow}$ are only dependent on this x coordinate. Note that the external field E does not contribute because it is taken independent of position and that the Seebeck terms are also gone in this equation. This is because the temperature gradient is taken constant in

our systems so that the gradients of $\nabla T_\uparrow$ and $\nabla T_\downarrow$ are both zero. In the next section I will explain a bit more about the spin dependent constants. It is known that in non-ferromagnetic metals, $\sigma_\uparrow = \sigma_\downarrow = \sigma$. This will make the equations solvable by hand for the N-side. Solving gives,

$$\mu_{\uparrow F}(x) = \frac{1}{2(\sigma_{\uparrow,F} + \sigma_{\downarrow,F})}[2\sigma_{\downarrow,F}(C_1 + C_2 x) + 2\sigma_{\uparrow,F}(C_3 + C_4 x) + e^{x/\lambda_F}\sigma_{\downarrow,F}(-C_1 - \lambda_F C_2 + C_3 + \lambda_F C_4)], \tag{11}$$

$$\mu_{\downarrow F}(x) = \frac{1}{2(\sigma_{\uparrow,F} + \sigma_{\downarrow,F})}[2\sigma_{\downarrow,F}(C_1 + C_2 x) + 2\sigma_{\uparrow,F}(C_3 + C_4 x) + e^{x/\lambda_F}\sigma_{\uparrow,F}(C_1 + \lambda_F C_2 - C_3 - \lambda_F C_4)], \tag{12}$$

$$\mu_{\uparrow N}(x) = \frac{C_5 x + C_6 + C_7 e^{x/\lambda_N} + C_8 e^{-x/\lambda_N}}{2}, \tag{13}$$

$$\mu_{\downarrow N}(x) = \frac{C_5 x + C_6 - C_7 e^{x/\lambda_N} - C_8 e^{-x/\lambda_N}}{2}, \tag{14}$$

which contains eight constants, C_1 through C_8, that have to be solved. The λ_{sr} are replaced for side-dependent relaxation lengths $\lambda_{N,F}$ because these relaxation lengths are dependent on the material. In the first two equations, all terms with e^{-x/λ_F} are thrown away because these blow up to ∞ when $x \to -\infty$. The same can be done for the equations of the N-side. If $x \to \infty$ the equation may not blow up, so terms with e^{x/λ_F} must vanish, therefor $C_7 = 0$. When this is done, you see that the equations at the F-side have the same form (except for the exponential terms) as the ones at the N-side when you add the $\sigma_{\uparrow,\downarrow,F}$ into these constants. Now that the formulas for $\mu_{\uparrow,\downarrow}$ are known, it can be solved with the help of the current densities j_e and j_s and some boundary conditions at the interface $x = 0$.

The system must go continuously from the F- to the N-side. Because our only boundary is at $x = 0$, all the boundary conditions are at $x = 0$. The first ones are not difficult to see. The charge and spin current densities are also split into two for the F- and N-side, just like the chemical potentials. Therefor we can say $j_{e,F}(0) = j_{e,N}(0)$ and $j_{s,F}(0) = j_{s,N}(0)$. For simplicity,

C_6 can be taken zero because it is an overall shift in $(\mu_{\uparrow,N} + \mu_{\downarrow,N})$. The same can be done for the F-side where C_1 and C_3 terms will take care of the overall shift. So if we take $\sigma_{\uparrow,F}C_1 = -\sigma_{\downarrow,F}C_3$, this shift will also be zero. We already have five boundary conditions, so we still need three to solve all eight.

The $\mu_{\uparrow,\downarrow}$ also have to go continuously. Note that these equations will not go smooth from the one to the other. There will be breaking which you can compare with the breaking of light when it hits a prism. The same is true for the current densities. The next equation will make sure all the $\mu_{\uparrow,\downarrow}$ will connect correctly from the F-side to the N-side,

$$\mu_{\uparrow F}(0) \pm \mu_{\downarrow F}(0) = \mu_{\uparrow N}(0) \pm \mu_{\downarrow N}(0). \tag{15}$$

The last boundary condition will come from the fact we do not want any charge current through our system. This results in a Peltier effect which we do not want in these simulations. Therefor $j_{e,N}(0) = j_{e,F}(0) = 0$. Now let's see how we can calculate the different spin-dependent constants in our system.

2.4 Calculation of spin-dependent constants

The majority of the constants we use are spin-dependent. Luckily, there are many known values and formulas.[5][6][7] The conductivity of a metal describes how it can resist electrical flow through it. When a metal has high conductivity, currents will go smoothly through the metal. It can be written as

$$\sigma_{\uparrow,\downarrow} = \frac{\sigma_{py}(1 \pm P_{\sigma_{py}})}{2}, \tag{16}$$

$$\sigma_{py} = \sigma_{\uparrow} + \sigma_{\downarrow}, \tag{17}$$

where σ_{py} is the conductivity of permalloy of $4.3 * 10^6\ S/m$.[5] For a table of all these known parameters, go to the Appendix at the end of this Thesis. Together with the conductivity polarization of Py,

$$P_{\sigma_{py}} = \frac{\sigma_{\uparrow} - \sigma_{\downarrow}}{\sigma_{\uparrow} + \sigma_{\downarrow}}, \tag{18}$$

which also has a known value of 0.25,[6] this conductivity problem can be solved. Note that this problem is only valid in the ferromagnetic region. In the non-ferromagnetic material $\sigma_\uparrow = \sigma_\downarrow = \sigma$ holds. The spin-dependent Seebeck coefficients are also found by this method. The only difference is that these coefficients are dependent on the conductivities,

$$S_{\uparrow,\downarrow} = S_{py} - \frac{(S_\uparrow - S_\downarrow)(P_{\sigma_{py}} \mp 1)}{2}, \tag{19}$$

$$S_{py} = \frac{\sigma_\uparrow S_\uparrow + \sigma_\downarrow S_\downarrow}{\sigma_{py}}, \tag{20}$$

$$P_{S_{py}} = \frac{S_\uparrow - S_\downarrow}{S_{py}}. \tag{21}$$

Seebeck coefficients describe the buildup of a voltage due to a temperature gradient throughout a material. The constants, S_{py} and $P_{S_{py}}$, are also experimentally known and have the following values respectively, $-20 * 10^{-6}$ V/K[7] and 0.19.[5] One can check, when using $P_{\sigma_{py}} = 0$ and $\sigma_\uparrow = \sigma_\downarrow$, one recovers $S_\uparrow = S_\downarrow = S$ in the non-ferromagnetic region. For convenience, the temperatures of the spin up and down electrons, $T_\uparrow$ and $T_\downarrow$, are equal. This is acceptable because in real experiments, "the spin-conserving inelastic scattering is on a scale much smaller than the device dimensions." [8] [p.21] With this theory done, we can start modelling!

3 Case 1: Spin-injection with a charge current

3.1 Without Seebeck terms

The first and simplest system will be the one without the Seebeck terms in the formulas for $j_\uparrow$ and $j_\downarrow$. That means there has to be something else to make spin-injection into the non-ferromagnetic region even possible. It can be done with use of a charge current density j_e. Normally, a electrical charge current will cause a Peltier effect to build up. This current will carry some heat which is described by Peltier coefficients. For consistency with the other cases, this will be ignored here.

A boundary condition will change with the addition of j_e. The charge current densities is non-zero now at the interface where normally (in all the next simulations) it is zero. This interface charge current density will look like $j_{e,N}(0) = j_{e,F}(0) = j_e$, with j_e assumed to be $1 * 10^9\ Am^{-2}$. It is taken this way so that we can compare this with the next case correctly. It is a realistic value so there should be no problem.[5] Finally the current densities will look like

$$j_{e,F} = -\sigma_\uparrow \frac{\nabla \mu_\uparrow}{e} - \sigma_\downarrow \frac{\nabla \mu_\downarrow}{e}, \tag{22}$$

$$j_{s,F} = -\sigma_\uparrow \frac{\nabla \mu_\uparrow}{e} + \sigma_\downarrow \frac{\nabla \mu_\downarrow}{e}, \tag{23}$$

$$j_{e,N} = -\sigma \frac{\nabla \mu_\uparrow}{e} - \sigma \frac{\nabla \mu_\downarrow}{e}, \tag{24}$$

$$j_{s,N} = -\sigma \frac{\nabla \mu_\uparrow}{e} + \sigma \frac{\nabla \mu_\downarrow}{e}, \tag{25}$$

and with the help of our boundary conditions, graphics can be made of the chemical potentials and the spin and charge current densities.

3.2 Application

All the graphics of our models will be presented in the Appendix. In the first figure for this case, Figure (3), we see the distribution of the chemical

potentials of the spin up and down electrons. At the F-side the electrons have a way shorter relaxation length (5 nm) than at the N-side (350 nm).[6] [9] [10] This can be seen in the figure. The difference between the chemical potentials of the spin up (blue line) and spin down (orange line) electrons is cut in half at the relaxation length which is expected. The green line represents the average chemical potential and is indeed a straight line what you would expect from the charge conservation law (9). After a couple of relaxation lengths, $\mu_\uparrow$ and $\mu_\downarrow$ will go to each other and reach equilibrium. The red line is described by

$$\mu_c = \frac{\sigma_\uparrow \mu_\uparrow + \sigma_\downarrow \mu_\downarrow}{\sigma_\uparrow + \sigma_\downarrow}, \tag{26}$$

and only holds for the F-side. Note that when we are at the N-side, $\sigma_\uparrow = \sigma_\downarrow = \sigma$, the average chemical potential (green line) is found. Because the two metals have different conductivities, there is a gap between this red line and the green line at the interface. This is used for measuring the spin accumulation μ_s.[11]

If we look at the spin and charge current densities in Figure (4), with j_s (blue line) and j_e (orange line), we see that j_e is just a constant through the whole material. This is preferred because if we add Seebeck terms later on and we set $j_e = 0$ because we do not want any current flow, a j_e of zero is expected everywhere. The spin current density j_s will change very rapidly at the ferromagnetic side but will relax at about two relaxation lengths, when $\mu_\uparrow$ will be about the same as $\mu_\downarrow$. At the N-side it will go to zero after a couple of relaxation lengths and it will stay there.

4 Case 2: Spin-injection with a thermal gradient

4.1 With Seebeck terms

For the second case we will look at what happens if we change the charge current for a temperature gradient through the materials. This temperature gradient will give rise to a Seebeck effect which will add Seebeck terms, i.e., terms proportional to temperature gradients, to the charge and spin current densities,

$$j_{e,F} = -\sigma_\uparrow \frac{\nabla \mu_\uparrow}{e} - \sigma_\downarrow \frac{\nabla \mu_\downarrow}{e} - \sigma_\uparrow S_\uparrow \nabla T - \sigma_\downarrow S_\downarrow \nabla T, \tag{27}$$

$$j_{s,F} = -\sigma_\uparrow \frac{\nabla \mu_\uparrow}{e} + \sigma_\downarrow \frac{\nabla \mu_\downarrow}{e} - \sigma_\uparrow S_\uparrow \nabla T + \sigma_\downarrow S_\downarrow \nabla T, \tag{28}$$

$$j_{e,N} = -\sigma \frac{\nabla \mu_\uparrow}{e} - \sigma \frac{\nabla \mu_\downarrow}{e} - \sigma S \nabla T - \sigma S \nabla T, \tag{29}$$

$$j_{s,N} = -\sigma \frac{\nabla \mu_\uparrow}{e} + \sigma \frac{\nabla \mu_\downarrow}{e} - \sigma S \nabla T + \sigma S \nabla T, \tag{30}$$

where again the ferromagnetic and the non-ferromagnetic sides are kept apart. Note that in (29) and (30) the two Seebeck terms can be added to or subtracted from each other.

4.2 Application

If we look at Figure (5), we see one big difference from the case without Seebeck terms, the slope of the chemical potentials. The reason is the Seebeck coefficient itself. At the F-side it is negative and at the N-side positive. The way the Seebeck coefficient is defined causes this. If S is positive, the side of the metal with the higher temperature has the lowest voltage, or in our case the lowest chemical potential. Because we defined ∇T to be positive (so to the left it is colder as to the right), the figure can be understood. At the N-side S is positive, so at the far right side of N, it has lower chemical potential than at the interface because it is warmer there. At the F-side this is turned around because the S there is negative. The relaxation lengths still

causes the chemical potentials to go to each other at relative long lengths just as the previous case.

In Figure (6), the charge current density j_e is zero everywhere which is exactly what we wanted. The spin current density j_s has the same shape as before. In Figure (11) the two spin current densities are shown from Case 1 and 2. It is clearly they follow the same pattern. This shows that spin-injection indeed can happen with a charge flow as well as a temperature gradient through the material. Now it is also clear why a value $j_e = 1 * 10^9\ Am^{-2}$ is taken for Case 1. If it was any lower, these figures will not be near each other. For the next cases, we will only compare them to this one because they all use a temperature gradient except for Case 1.

In the figures for the spin current density, we see it transports spin current to the non-ferromagnetic region. Because there is no external magnetic field, the spin particles will not align with it and they stay roughly how they are. With this, one can try to store data. In 2007, the Nobel prize was given to A. Fert and P. Grünberg for discovering the GMR (Giant Magnetoresistance) effect which describes how the electrical resistance fades due to a applied magnetic field in multi layered ferromagnetic systems. This effect is used in every hard drive nowadays and it is subject to lots of research for better utilization and new spin based concepts.

All coupled spin, charge and heat (which is ignored here) transport were understood with equal temperatures for spin up and down electrons. With the heat current experiment of Dejene *et al*, it is shown there is a temperature difference between spin up and down electrons of around 120 mK at room temperature which is around 10% of the total temperature gradient through the system.[12] The technique described in this article to measure the temperature difference allows the study of inelastic spin scattering at any temperature. This was not doable before that time. In this Thesis, scattering is completely ignored (aside from a magnon scatter term in the next case), even though it is a really important feature, since electrons may scatter with magnons if they are added into the equation.

5 Case 3: Introducing Magnons

In the next scenario, there will only be magnons at the ferromagnetic side of the system. There is currently a lot of research going on to fully understand the role of magnons in magnetic insulators. Because the vast complexity of describing magnons, the majority of the formulas[13] presented here are assumptions and simplifications. The N-side has only electrons, just like before.

5.1 Magnon drag terms

First, we assume magnons propagate with a certain magnon spin propagation length λ_m. The relation between this and the chemical potential is similar to the spin up and down electrons,

$$\nabla^2 \mu_m = \frac{\mu_m}{\lambda_m^2}. \tag{31}$$

This differential equation leads to an equation for μ_m and can be simplified further,

$$\mu_m(x) = C_9 e^{x/\lambda_m} + C_{10} e^{-x/\lambda_m} \tag{32}$$

where we introduced two new integration constants, C_9 and C_{10}. Magnons will only appear at the ferromagnetic side, which is the left side of our system, so when x reaches $-\infty$, the magnon chemical potential may not go to ∞. Therefore C_{10} must be zero. At the non-ferromagnetic side, things are still the same and formulas (13) and (14) still hold. With the addition of magnons, the currents also change. An extra term contributes to the spin current density,

$$j_{s,F} = j_{\uparrow,F} - j_{\downarrow,F} - \sigma_s \frac{\nabla \mu_m}{\hbar} \frac{2e}{\hbar} - L \nabla T \frac{2e}{\hbar}, \tag{33}$$

where σ_s is the magnon spin conductivity of the magnet and L the bulk spin Seebeck coefficient. These extra terms are called magnon drag terms and describe transport from the ferromagnetic to the non-ferromagnetic region. To make everything in units of Am^{-2}, a factor $2e/\hbar$ is added to these new terms.

In this section, there are no electrons at all at the side where the magnons are, so $j_{\uparrow,F}$ and $j_{\downarrow,F}$ can be ignored entirely just as $j_{e,F}$. Formula (29) and (30) still hold for the N-side of the system. Together with this new current density, there will also be a new boundary condition,

$$j_{s,m}(0) = \frac{3g_{\uparrow\downarrow}}{2s\pi\Lambda^3}\frac{2e}{\hbar}(\mu_m(0) - \mu_s(0)). \tag{34}$$

At the interface, this relation holds between the different chemical potentials with the help of the spin mixing conductance $g_{\uparrow\downarrow}$. It describes the efficiency of spin transport through the interface. For Py/Cu systems, this constant is around 5 nm^{-2}. One thing to note is that this constant is dependent on the thickness of the materials used[14] which is ignored here entirely. The spin density s will assumed to be proportional to a^{-3} where a is the lattice constant which is around 0.3 nm.[15]

These new constants due to the addition of magnons can be found with so-called relaxation time approximation formulas and look like this,

$$\sigma_s \sim \frac{J_s\tau}{\Lambda^3}, \tag{35}$$

$$L \sim \frac{J_s\tau k_B}{\hbar\Lambda^3}, \tag{36}$$

$$\lambda_m \sim v_m\sqrt{\tau\tau_{sr}}, \tag{37}$$

where they all depend on relaxation times τ_{sr}, which is the magnon spin relaxation time, and τ. This time τ originates from many different scattering processes, which is something that needs further research. For now, lets assume both time scales are proportional to

$$\tau_{sr} \sim \tau \sim \frac{\hbar}{\alpha k_B T}, \tag{38}$$

with α being the Gilbert damping constant which is around 0.01[16] for our system. The two other constants,

$$v_m = \frac{2\sqrt{J_s k_B T}}{\hbar}, \tag{39}$$

$$\Lambda = \sqrt{\frac{4\pi J_s}{k_B T}}, \tag{40}$$

are the magnon thermal velocity and the DeBroglie wavelength for magnons respectively. Here, J_s is the spin stiffness which comes from the dispersion relation for magnons $\hbar\omega_{\vec{k}} = J_s k^2$ where magnons have a wave vector $\vec{k}$. For this constant $4 * 10^{-40}\ Jm^2$ is used.[17] If we plug these new constants into (33), we see that the new terms are also in units of Am^{-2}.

5.2 Application

With the use of these new conditions and constants, the figures once again can be made. In Figure (7), the magnon chemical potential is displayed as a black line. With the help of (37), we see that $\lambda_m = 62.1535 * 10^{-9}\ m$. The strength of this magnon effect is strongest at the interface and quickly dissipates after two magnon relaxation lengths. At the N-side, the two chemical potentials, $\mu_\uparrow$ and $\mu_\downarrow$, have switched places. This is just because we defined magnons this way, to have negative magnon drag terms in formula (33) for the spin current density. The slope is still the same at the N-side.

Because there are no electrons at the side of the magnons, the spin current density j_s in Figure (8) looks a bit different. It is negative now, just as with the chemical potentials, but it still follows the same pattern. At the N-side, the two individual terms are also plotted, $-L\nabla T\frac{2e}{\hbar}$ in red and $-\sigma_s \nabla \mu_m \frac{2e}{\hbar^2}$ in green. The spin current density goes to zero again at relative big values for x. This shows that if magnons plays the only roll at the ferromagnetic side, and they describe the formulas above, there still can be spin-injection into the non-ferromagnetic region.

6 Case 4: Magnons and Electrons

6.1 All terms

Last, a system with magnons and electrons will be simulated at the ferromagnetic region. The non-ferromagnetic side is taken the same as usual. For clarity, the spin and charge current densities will be given again,

$$j_{e,F} = -\sigma_\uparrow \frac{\nabla \mu_\uparrow}{e} - \sigma_\downarrow \frac{\nabla \mu_\downarrow}{e} - \sigma_\uparrow S_\uparrow \nabla T - \sigma_\downarrow S_\downarrow \nabla T, \tag{41}$$

$$j_{s,F} = -\sigma_\uparrow \frac{\nabla \mu_\uparrow}{e} + \sigma_\downarrow \frac{\nabla \mu_\downarrow}{e} - \sigma_\uparrow S_\uparrow \nabla T + \sigma_\downarrow S_\downarrow \nabla T - \sigma_s \frac{\nabla \mu_m}{\hbar} \frac{2e}{\hbar} - L \nabla T \frac{2e}{\hbar}, \tag{42}$$

$$j_{e,N} = -\sigma \frac{\nabla \mu_\uparrow}{e} - \sigma \frac{\nabla \mu_\downarrow}{e} - \sigma S \nabla T - \sigma S \nabla T, \tag{43}$$

$$j_{s,N} = -\sigma \frac{\nabla \mu_\uparrow}{e} + \sigma \frac{\nabla \mu_\downarrow}{e} - \sigma S \nabla T + \sigma S \nabla T. \tag{44}$$

Note that in (43) and (44) the two Seebeck terms can be simplified again.

6.2 Application

The chemical potentials in Figure (9) once again have the same shape as in Case 2, but there is a difference now at the interface. In Case 3 we saw that μ_m was pretty large while here, the energy is divided between the electrons and the magnons. The magnons still seems to be the most important contribution at the interface.

In Figure (10), the spin charge current is plotted again. This time, it is a superposition of the spin current density of the electrons (purple) and the magnons (green and red). The charge current density j_e is once again zero everywhere. Here we also see that the spin current density coming from the $-\sigma_s \nabla \mu_m \frac{2e}{\hbar^2}$ term (green) has decreased significantly. It also looks more like the spin current we had in Case 2 but negative, in comparison with Case 3, where we only had magnons at the F-side.

7 Temperature-dependent Seebeck coefficient

A nice addition to these models, is to see in what way they are temperature dependent and in what temperature regime electrons and magnons are important. To do this we want to know how the spin accumulation at the interface, $\mu_s = \mu_{\uparrow,N}(0) - \mu_{\downarrow,N}(0)$, will look like when this temperature is variable. One way to do this is with the Mott relation for the Seebeck coefficients where a Fermi electron gas is assumed,

$$S(T) \sim \frac{\pi^2 k_B}{3e} \frac{T}{T_F}, \tag{45}$$

$$T_F = \frac{\hbar^2}{2m_e k_B} (3\pi^2 n)^{2/3}, \tag{46}$$

with the right unit for the Seebeck coefficient of V/K and the Fermi temperature T_F of the metal used. This T_F is the temperature when electrons in a gas or metal are significantly faster than at absolute zero. Even at this zero kelvin, fermions, like electrons, are moving at Fermi velocity. In metals, the Fermi temperature is $\sim 10^5\ K$. The Seebeck coefficient is different for each metal, so is T_F due to its dependence of the electron density n with electron rest mass is m_e.

For metals, n is $\sim 10^{28} m^{-3}$.[18] So for Py the electron density for iron will be used for simplicity. Iron and nickel will have quite the same n. In the Appendix, the electron densities of the different metals are displayed.

The temperature-dependence of the conductivities is relatively small, so it will be ignored here. If these new Seebeck coefficients are put into our models, one can hopefully see in what temperature regimes magnons and electrons are important. One thing to note, the melting points for these metals will be at 1300K and higher, so T will only run from 0K to 1300K.

One thing is pretty clear in Figure (12). If we look at Case 2 (blue line, only electrons at F-side), the spin accumulation μ_s is way smaller than in the other cases. It is just a positive straight line going up and around 100 times smaller. The red line describes the μ_s of Case 3 (only magnons at F-side) and the purple line the one of Case 4 (electrons and magnons at F-side).

Note that the blue and the purple line are the most complete models. If the blue line was around the same order of magnitude, the purple line is what you would expect, just the contribution of the blue (electrons) and the red (magnons) line. The pink line is just the average of the red and blue line for comparison.

If we look at the values for our new Seebeck coefficients at room temperature with equation (45), $S_{Cu}(300K) = 1.04199 * 10^{-6}$ and $S_{Py}(300K) = -6.54869 * 10^{-7}$, we see they are not the same as we saw before. The Seebeck coefficient for copper should be around 1.6 times bigger and the one for permalloy 30 times. Even if we add these factors into the equation, the blue line in Figure (12) is still around 100 times smaller then the others. There is a noticeable increase at higher temperatures though. If we simplify the formulas for these μ_s we can see what dependence they have in T. The μ_s of cases 2, 3 and 4 are

$$\mu_{s,2} = aT, \tag{47}$$

$$\mu_{s,3} = \frac{-bT}{c + d\sqrt{T} + eT\sqrt{T}}, \tag{48}$$

$$\mu_{s,4} = \frac{fT - g\sqrt{T}}{h + iT + j/\sqrt{T}}, \tag{49}$$

where a through j replaced the constants to make it more clearly. It becomes very complex with the addition of magnons. With this information I cannot conclude in what temperature regimes magnons and electrons are important. One thing I can say is, if we look at Figure (12), the magnon lines grows way faster than just linearly. So my expectation is that magnons are very important at low temperatures, but it becomes less important when a couple of hundred kelvin is reached. At zero kelvin, the spin accumulation is in every case zero. For the case of magnons it is no surprise. At zero kelvin all the spin particles are perfectly aligned (no deviations from each other), so no spin-waves or magnons can exist because they depend on these deviations.

The reason why the spin accumulation is zero in the case of electrons, is also this perfect alignment. At zero kelvin the system is in ground state with the lowest energy possible. This lowest energy can only be reached if all spin particles are aligned (Ising Model). This means there is only one species,

only up spins or only down spins. This will lead to $\mu_s = 0$ at zero kelvin. As a remark, spin-injection due to a temperature gradient is also a bit weird if we look at zero kelvin at the interface. The temperature gradient goes from the left metal to the right. If the interface is at zero kelvin, one metal has to be zero kelvin everywhere, which means spin-injection is impossible without a charge or heat current.

8 Comparison and Conclusion

In this Thesis, different cases are modelled to see what spin-injection is and what happens when magnons are added into the system. We showed spin-injection can be achieved due to a charge current and a temperature gradient. We started with a system without Seebeck coefficients (Case 1) where the spin-injection was achieved with a charge current. This charge current is zero for the other cases where spin-injection was accomplished with a constant temperature gradient through the system. First, only electrons (Case 2) were assumed at the ferromagnetic side, then only magnons (Case 3) and finally both (Case 4). Although it is not really realistic to only have magnons at one side because they need spin particles as a kind of medium to exist, it is interesting to see how magnons alone alter the system.

8.1 Results

Cases 2, 3 and 4 have a important similarity, namely the way the electrons go to equilibrium at some material relaxation length. If their equations are compared, you see they all go exactly to the same equilibrium at a certain length. This is seen by the average chemical potential $(\mu_\uparrow + \mu_\downarrow)/2$. At the ferromagnetic side, in cases 2 and 4 (3 has no electrons at F-side) they go to $1.28176 * 10^{-16}x$ and at the non-ferromagnetic side, in cases 2, 3 and 4, they go to $-1.025408 * 10^{-17}x$. A noticeable difference occurs when magnons are added into the system in Case 3 and 4. The chemical potentials of the up and down electrons switch places. This happens because we defined magnons in a certain way. The spin current also goes from positive to negative if we add magnons.

The spin accumulation μ_s is another thing that can tell us more about the models. This spin accumulation is the difference between the chemical poten-

tials. Because the magnons switch these two, I will take the absolute value of it. In Case 2, we see a μ_s of $9.33252 * 10^{-26}$ J. When we replace the electrons to magnons in Case 3, we get a increase to $1.08229 * 10^{-23}$ J. The most interesting thing is the magnon chemical potential at the interface $\mu_m(0)$. This is exactly the same as the spin accumulation. The same thing happens in Case 4 with magnons and electrons, where μ_s and $\mu_m(0)$ are $3.24932 * 10^{-24}$ J. So with the addition of magnons, the spin accumulation becomes bigger.

If the spin currents are compared, one sees aside from it being negative, the same pattern. At the ferromagnetic side, relatively far from the interface, electrons are in equilibrium and have a constant spin current. Reaching the interface, the spin current is going to the non-ferromagnetic side due to the temperature gradient, and goes to zero at large x. In real systems this happens due to scattering which mainly comes from phonons (lattice vibrations). The added magnon drag and the electron terms are of the same order of magnitude. But in Case 4 one sees a smaller contribution from the first magnon term (green lines Figures (8) and (10)). One thing to note is that the formulas for σ_s and L do not have exact values. A factor of 2 to one of them will change the whole spin current.

In addition to this, it is interesting to see how effective the spin-injection is. This is only viable for Case 2 and 4 because these are the most complete systems described in the Thesis. If we take the current spin density at the interface in both cases, and divide them by the current spin density at equilibrium (just a big negative number for x), you get how much percentage of the spin current is left at the beginning of the non-ferromagnetic region. For Case 2 this is 23,36% and for Case 4 this is 21,09%. This is a bit odd because one would expect that it would be higher when magnons are added. Although no scattering between electrons and magnons is described, one can imagine electrons are pushed a bit due to the addition of spin waves which results in a higher spin-injection. Because this spin current is negative, but has positive terms, this may influence the effectiveness. It is also interesting to see that the spin current coming from the electrons (purple line Figure (10)) is going up if it reaches the interface. In Case 2 it went down. This probably has to do with the magnon drag terms being negative. The result is pretty similar though to Case 2.

Finally we described how the spin-injections are dependent on the temperature if we make the Seebeck coefficient temperature dependent. The question is in what temperature range electrons and magnons are important. One way to do that is with the spin accumulation at the interface $x = 0$. We saw that the calculated Seebeck coefficients for Cu and Py differ with a factor 1.6 and 30. Even with these factors, μ_s of Case 2 (without magnons) is $\sim 10^2$ times smaller than the μ_s of cases 3 and 4. This is mentioned earlier in this section. One thing that was as expected was the purple line in Figure (12) which represents Case 4 (electrons and magnons). It is in between the red(magnons) and the blue(electrons) line. Because the blue line is significantly smaller than the others, no good answer can be given to our question. The only thing you can say is that the magnon lines go really steeply just above zero kelvin, which imply the magnon drag terms are important at very low temperatures. At zero kelvin, all μ_s go to zero. For the magnons this is right because at 0K, there are no deviations from the alignment of the spin, so there are no magnons. For electrons, zero kelvin means all electrons are in the ground state and have the same alignment. This means there is only one species of spin, up or down, which leads to no spin accumulation at zero kelvin.

8.2 Discussion

With this, it can be said that the contribution of magnons seems too high in comparison with the electrons. The idea was to add magnon terms to a well-defined system, which probably will lead to small corrections. This is clearly not the case. This is probably due to the vast number of assumptions and simplifications. We started with the assumption that the external electrical field E is zero. This cannot be true because a ∇T will cause an electric field in the conductor.[19] Mentioned before, the temperature difference between the spin up and down electrons can be up to 10 % of the total temperature gradient throughout the system.[12]

Other flaws can be traced back with the addition of magnons. The Gilbert damping constant α is dependent on the atomic magnetization and the thickness of the material.[16] This can range from 0.001 to 0.1. We also ignored magnon drag terms for the charge current density. One can make similar looking magnon drag terms for j_e with a $\nabla \mu_m$ term and one with a ∇T term with different constants than the drag terms already used. The system also

looks very different when the materials have a certain thickness. You cannot throw away terms anymore and extra exponential terms shows up with extra boundary conditions.

With a lot of research going on now in the field of spintronics and magnons, the motivation was present to make this Thesis. There surely is room for improvements and expansion of these simulations to systems with finite thickness for example. Because of major potential for spintronic based devices and quantum computing, this field of research must be expanded and supported.

9 Appendix

9.1 Parameters

Constant	Discription	Used Value	Unit
$\lambda_{Cu} = \lambda_N$	Spin relaxation length in Cu	[6][10]350	nm
$\lambda_{Py} = \lambda_F$	Spin relaxation length in Py	[6] [9] [10]5	nm
σ_{Cu}	Conductivity of Cu	[5]$43 * 10^6$	S/m
σ_{Py}	Conductivity of Py	[5]$4.3 * 10^6$	S/m
$\sigma_{\uparrow}$	Conductivity of $\uparrow$ electrons in Py	$2.6875 * 10^6$	S/m
$\sigma_{\downarrow}$	Conductivity of $\downarrow$ electrons in Py	$1.6125 * 10^6$	S/m
S_{Cu}	Seebeck coefficient of Cu	[7]$1.6 * 10^{-6}$	V/K
S_{Py}	Seebeck coefficient of Py	[7]$-20 * 10^{-6}$	V/K
$S_{\uparrow}$	Seebeck coef. of $\uparrow$ electrons in Py	$-21.425 * 10^{-6}$	V/K
$S_{\downarrow}$	Seebeck coef. of $\downarrow$ electrons in Py	$-17.625 * 10^{-6}$	V/K
P_{σ}	Conductivity polarization in Py	[6][10]0.25	
P_S	Seebeck polarization in Py	[5]0.19	
T	Temperature	300	K
∇T	Temperaturegradient	[20]$4 * 10^7$	K/m
j_e	Constant charge current density	$1 * 10^9$	A/m^2
k_B	Boltzmann constant	[21]$1.3806 * 10^{-23}$	J/K
$\hbar$	Reduced Planck constant	[21]$1.0546 * 10^{-34}$	Js
e	Elementary charge	[21]$1.6022 * 10^{-19}$	C

Table 1: Various constants used in the models described above. Spin up and down conductivities and Seebeck coefficients are calculated with formulas in this Thesis.

Constant	Discription	Used Value	Unit
m_e	Electron rest mass	$^{[21]}9.1095 * 10^{-31}$	kg
n_{Fe}	Electron density in iron	$^{[18]}17 * 10^{28}$	m^{-3}
n_{Cu}	Electron density in copper	$^{[18]}8.47 * 10^{28}$	m^{-3}
S_{Cu}	Calculated Seebeck coef. Cu	$1.04199 * 10^{-6}$	V/K
S_{Py}	Calculated Seebeck coef. Py	$-0.654869 * 10^{-6}$	V/K
$g_{\uparrow\downarrow}$	Spin mixing conductance	$^{[14]}5 * 10^{18}$	m^{-2}
J_s	Spin stiffness	$^{[17]}4 * 10^{-40}$	Jm^2
α	Gilbert demping constant	$^{[16]}0.01$	
a	Lattice constant	$^{[15]}0.3$	nm
Λ	DeBroglie wavelength magnons	1.10164	nm
λ_m	Magnon spin prop. length	62.1535	nm
L	Bulk spin Seebeck coefficient	$9.97281 * 10^{-14}$	$Jm^{-1}K^{-1}$
σ_s	Spin conductivity	$7.61794 * 10^{-25}$	Js/m

Table 2: Various constants used in the models to describe magnons. The calculated Seebeck coefficients are calculated with (45) at room temperature. The four lowest constants are calculated with formulas in this Thesis.

9.2 Figures

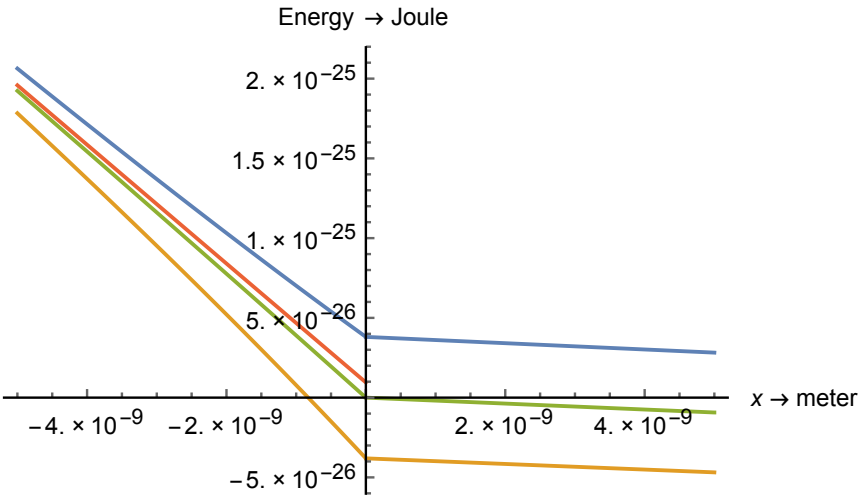

Figure 3: **Case 1**. In blue and orange, the chemical potentials $\mu_\uparrow$ and $\mu_\downarrow$ are plotted. And in green and red, the average $(\mu_\uparrow + \mu_\uparrow)/2$ and μ_c are plotted.

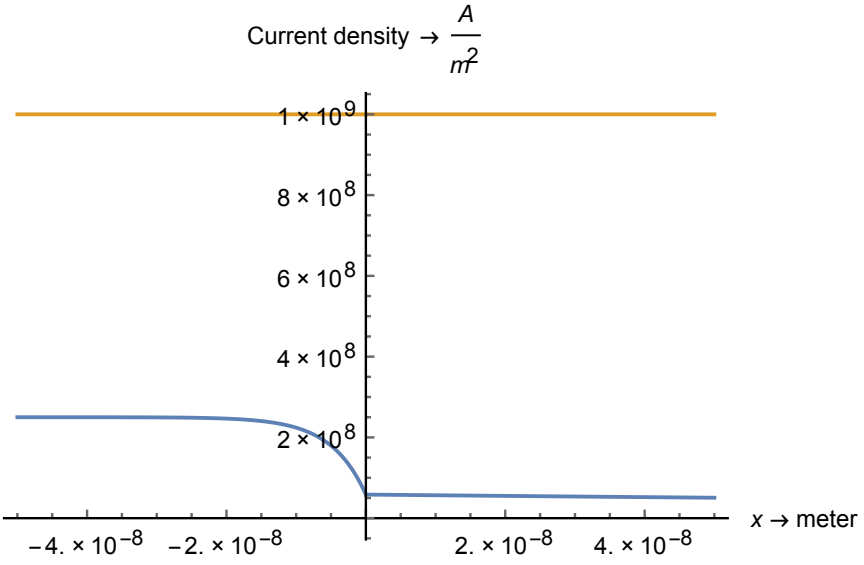

Figure 4: **Case 1**. In blue, the spin current density j_s is plotted. In orange the charge current density j_e is plotted and is equal to $j_e = 10^9$ everywhere.

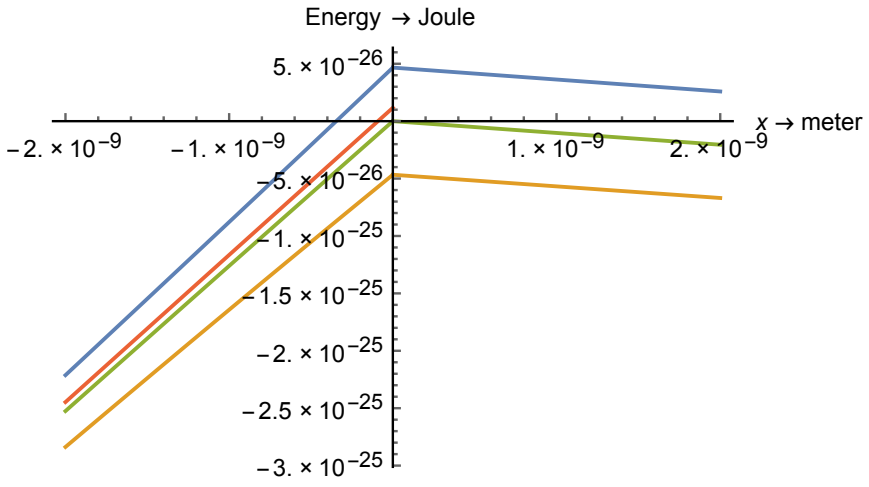

Figure 5: **Case 2**. In blue and orange, the chemical potentials $\mu_\uparrow$ and $\mu_\downarrow$ are plotted. And in green and red, the average $(\mu_\uparrow + \mu_\uparrow)/2$ and μ_c are plotted.

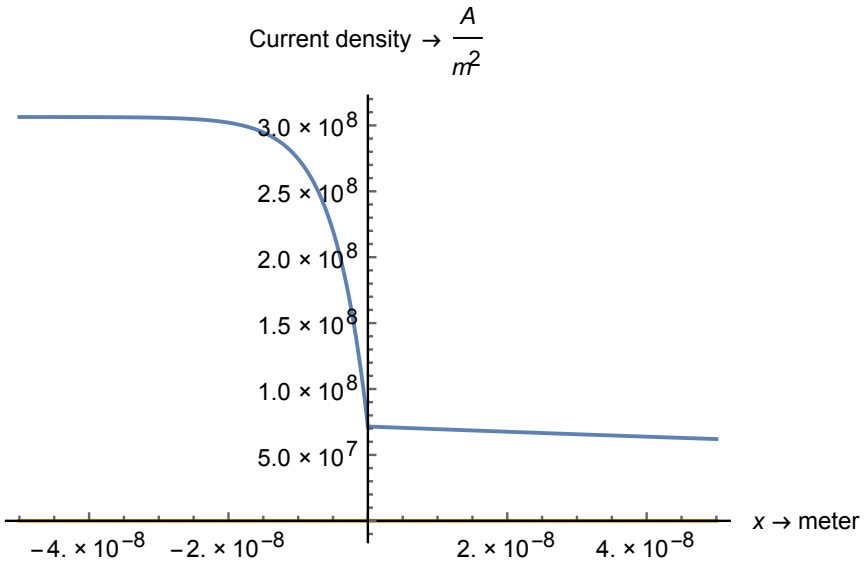

Figure 6: **Case 2**. In blue, the spin current density j_s is plotted. In orange the charge current density j_e is plotted and is zero everywhere as expected.

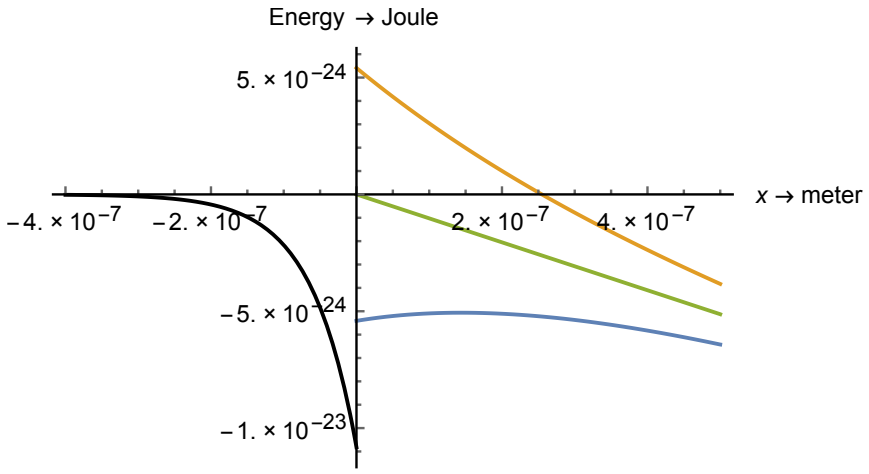

Figure 7: **Case 3**. In blue and orange, the chemical potentials $\mu_\uparrow$ and $\mu_\downarrow$ are plotted. And in green and black, the average $(\mu_\uparrow + \mu_\uparrow)/2$ and μ_m are plotted. Note the change of positions of $\mu_\uparrow$ and $\mu_\downarrow$.

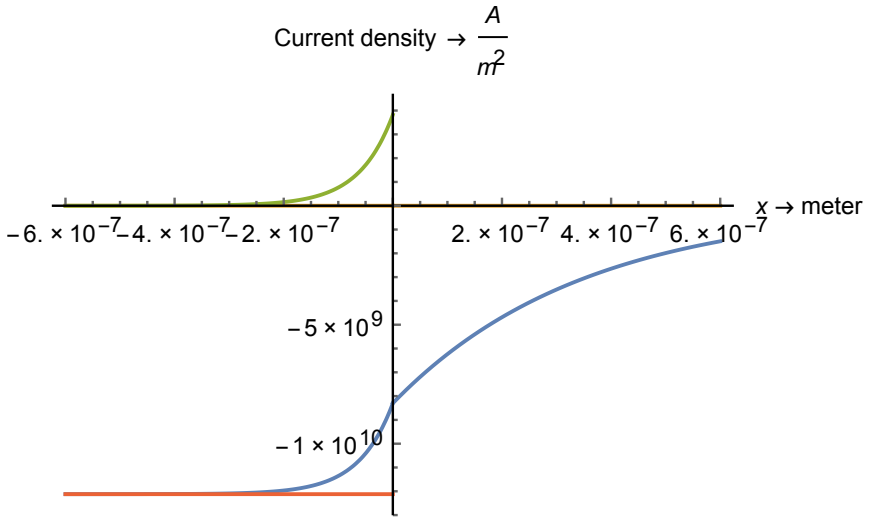

Figure 8: **Case 3**. In blue, j_s is plotted which is a combination of $-L\nabla T\frac{2e}{\hbar}$ (red) and $-\sigma_s \nabla \mu_m \frac{2e}{\hbar^2}$ (green). In orange the charge current density j_e is plotted and is zero everywhere as expected.

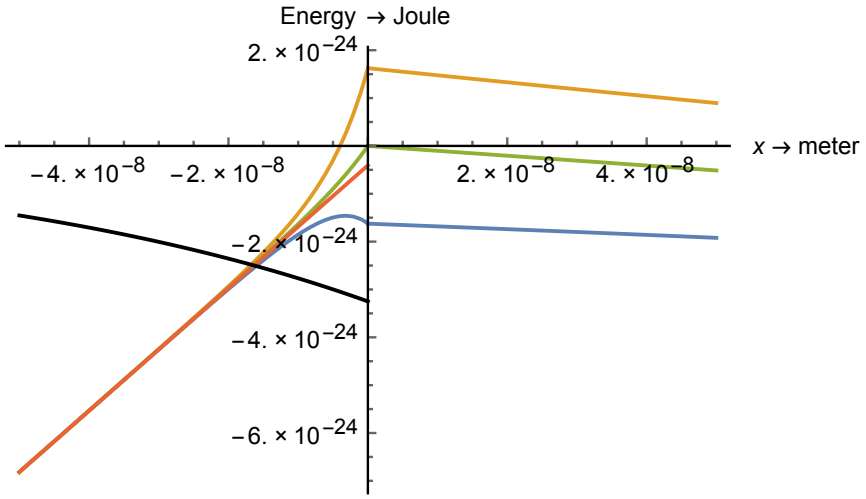

Figure 9: **Case 4**. In blue and orange, $\mu_\uparrow$ and $\mu_\downarrow$ are plotted. And in green, red and black, $(\mu_\uparrow + \mu_\uparrow)/2$, μ_c and μ_m are plotted.

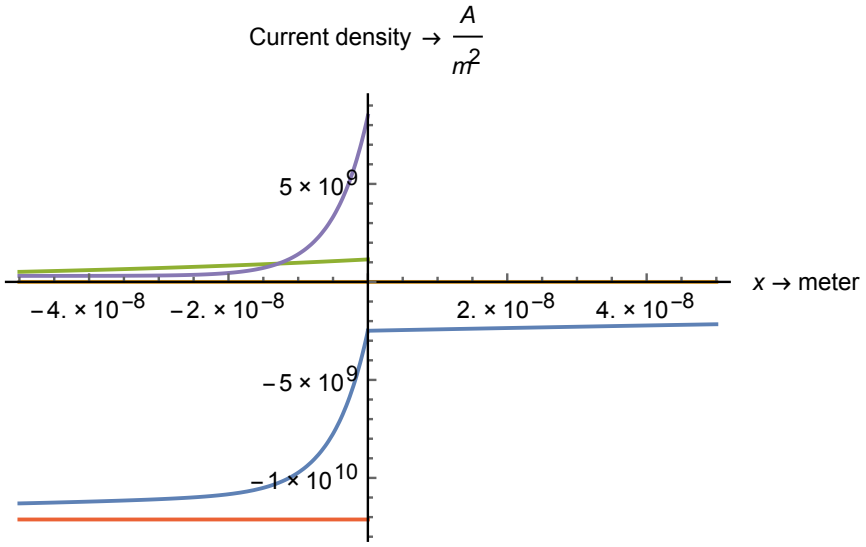

Figure 10: **Case 4**. In blue, j_s is plotted which is the superposition of the contribution of the electrons (purple), and magnons which consists of $-L\nabla T\frac{2e}{\hbar}$ (red) and $-\sigma_s\nabla\mu_m\frac{2e}{\hbar^2}$ (green). In orange, $j_e = 0$ again everywhere.

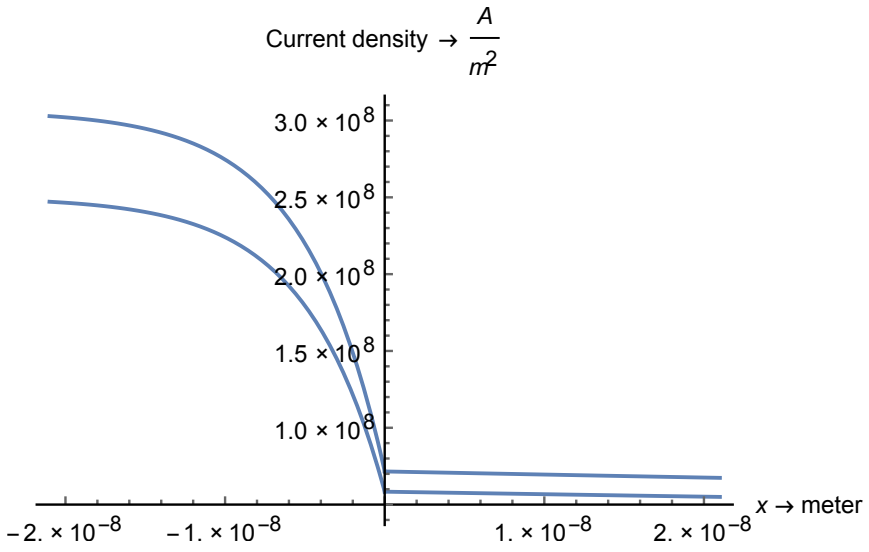

Figure 11: Spin current due to a charge current and a temperature gradient.

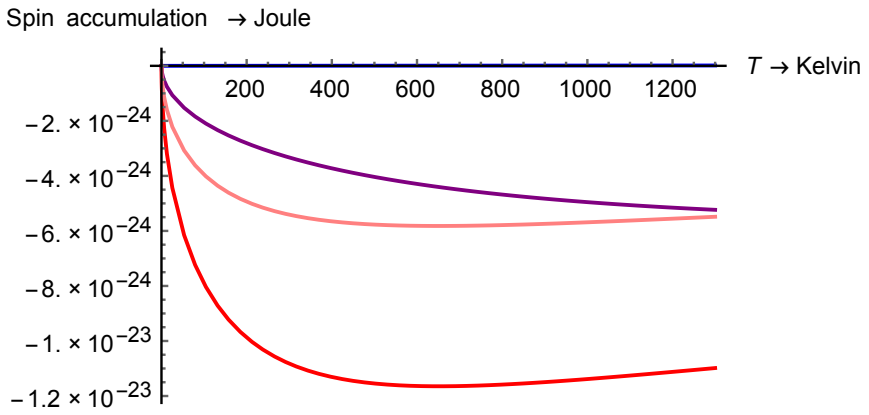

Figure 12: T-dependence of μ_s in the different cases described in this Thesis. The blue line (Case 2) is significantly smaller than the red (Case 3), purple (Case 4) and pink line (average of the blue and red line).

References

[1] I. Žutić, J. Fabian, S. Das Sarma, *Spintronics: Fundamentals and applications*, 2004, Reviews of Modern Physics 76, p. 323.

[2] T. Koga Y. Sekine, *Electron spin rotation and quantitative determination of spin-orbit coefficients*, 2012, NTT Technical Rev. Vol.10 No.9.

[3] A. Aronov, *Spin injection in metals and polarization of nuclei*, 1976, JEPT Lett. 24, p.32.

[4] T. Valet, A. Fert, *Theory of the perpendicular magnetoresistance in magnetic multilayers*, 1993, Phys. Rev. B 48, p. 7099.

[5] A. Slachter, F.L. Bakker, J.P. Adam, B.J. van Wees, *Thermally driven spin injection from a ferromagnet into a non-magnetic metal*, 2010, Nature 6, p. 879-882.

[6] F.L. Bakker, A. Slachter, J.P. Adam, B.J. van Wees, *Interplay of Peltier and Seebeck effects in nanoscale nonlocal spin valves*, 2010, Phys. Rev. Lett. 105, 136601.

[7] K. Uchida, S. Takahashi, K. Harii, J. Ieda, W. Koshibae, K. Ando, S. Maekawa, E. Saitoh, *Observation of the spin Seebeck effect*, 2008, Nature 455, p. 778-781.

[8] F.L. Bakker, *Thermoelectric effects in magnetic nanostructures*, 2012, Zernike Institute PhD Thesis, University of Groningen.

[9] S. Dubois, L. Piraux, J.M. George, K. Ounadjela, J.L. Duvail, A. Fert, *Evidence for a short spin diffusion length in permalloy from the giant magnetoresistance of multilayered nanowires*, 1999, Phys. Rev. B 60, p. 477.

[10] F.J. Jedema, A. Filip, B.J. van Wees, *Electrical spin injection and accumulation at room temperature in an all-metal mesoscopic spin valve*, 2001, Nature 410, p. 345-348.

[11] P.V. Son, H.V. Kempen, P. Wyder, *Boundary resistance of the ferromagnetic-nonferromagnetic metal interface*, 1987, Phys. Rev. Let. 58, p. 2271.

[12] F.K. Dejene, J. Flipse, G.E.W. Bauer, B.J. van Wees, *Spin heat accumulation and spin-dependent temperatures in nanopillar spin valves*, 2013, Nature 9, p. 636639.

[13] R.A. Duine, A Brataas, S.A. Bender, Y. Tserkovnyak, *Spintronics and Magnon Bose-Einstein Condensation*, May 6th 2015.

[14] P. Deorani, H, Yang, *Role of spin mixing conductance in spin pumping: enhancement of spin pumping efficiency in Ta/Cu/Py structures*, 2013.

[15] M.E. Lucassen, C.H. Wong, R.A. Duine, Y. Yserkovnyak, *Spin-transfer mechanism for magnon-drag thermopower*, 2011, Applied Phy. Let. 99, 262506.

[16] Y. Tserkovnyak, A. Brataas, G.E.W. Bauer, *Enhanced Gilbert Damping in Thin Ferromagnetic Films*, 2002, Phys. Rev. Lett. 88, 117601.

[17] Y. Hsu, L. Berger, *Transport of heat by spin waves in* $Fe_{95}Si_5$, 1978, Phys. Rev. B 18, 4856.

[18] R.W.G. Wyckoff, *Crystal Structures* 2nd ed., 1963, Interscience, New York.

[19] N.F. Mott, H. Jones, *The Theory of the Properties of Metals and Alloys*, 1936, Oxford University Press.

[20] F.K. Dejene, J. Flipse, B.J. van Wees, *Spin-dependent Seebeck coefficients of* $Ni_{80}Fe_{20}$ *and* Co *in nanopillar spin valves*, 2012, Zernike Institute for Advanced Materials, University of Groningen, The Netherlands.

[21] N.W. Ashcroft, N.D. Mermin, *Solid State Physics*, 1976, Brooks/Cole, Cengage Learning.